Developmental Cell *10*, 367–377, March, 2006 ©2006 Elsevier Inc. DOI 10.1016/j.devcel.2006.02.010

Multiple Wnts and Frizzled Receptors Regulate Anteriorly Directed Cell and Growth Cone Migrations in *Caenorhabditis elegans*

Chun-Liang Pan,[1] James Endres Howell,[1,5] Scott G. Clark,[2,3] Massimo Hilliard,[2,4] Shaun Cordes,[1] Cornelia I. Bargmann,[2,4] and Gian Garriga[1,*]

[1] Helen Wills Neuroscience Institute and Department of Molecular and Cell Biology University of California, Berkeley Berkeley, California 94720

[2] Departments of Anatomy, and Biochemistry and Biophysics University of California, San Francisco San Francisco, California 94143

[3] Molecular Neurobiology Program Department of Pharmacology Skirball Institute NYU School of Medicine New York, New York 10016

[4] Howard Hughes Medical Institute The Rockefeller University 1230 York Avenue New York, New York 10021

Summary

A set of conserved molecules guides axons along the metazoan dorsal-ventral axis. Recently, Wnt glycoproteins have been shown to guide axons along the anterior-posterior (A/P) axis of the mammalian spinal cord. Here, we show that, in the nematode *Caenorhabditis elegans*, multiple Wnts and Frizzled receptors regulate the anterior migrations of neurons and growth cones. Three Wnts are expressed in the tail, and at least one of these, EGL-20, functions as a repellent. We show that the MIG-1 Frizzled receptor acts in the neurons and growth cones to promote their migrations and provide genetic evidence that the Frizzleds MIG-1 and MOM-5 mediate the repulsive effects of EGL-20. While these receptors mediate the effects of EGL-20, we find that the Frizzled receptor LIN-17 can antagonize MIG-1 signaling. Our results indicate that Wnts play a key role in A/P guidance in *C. elegans* and employ distinct mechanisms to regulate different migrations.

Introduction

During early development, neurons and their growth cones often migrate extensively, responding to various attractive or repulsive molecules in the environment, and reaching their destinations by a highly coordinated pattern of responses to these guidance cues. Many guidance molecules that regulate these cell and growth cone migrations have been discovered in the past two decades, and often they are conserved among species as diverse as nematodes, insects, and vertebrates (Dickson, 2002; Tessier-Lavigne and Goodman, 1996). The conserved cue UNC-6/Netrin, for example, guides the ventral growth of *C. elegans*, *Drosophila*, and vertebrate axons through its receptor UNC-40/Frazzled/DCC (Chan et al., 1996; Keino-Masu et al., 1996; Kennedy et al., 1994; Kolodziej et al., 1996; Mitchell et al., 1996; Serafini et al., 1994; Wadsworth et al., 1996). While a picture of how these cues guide axons along the dorsal-ventral (D/V) axis has emerged, our understanding of anterior-posterior (A/P) guidance is less clear. Recent studies, however, suggest that members of the Wnt glycoprotein family can be such A/P guidance cues (Liu et al., 2005; Lyuksyutova et al., 2003).

Wnts are a family of secreted glycoproteins found in all metazoans (Wodarz and Nusse, 1998). Like other morphogens such as Sonic hedgehog (Shh) and bone morphogenetic proteins (BMPs), Wnt gradients can be critical in organizing body patterns (Zecca et al., 1996). In *C. elegans*, Wnts play an important role in regulating asymmetric cell divisions (Herman et al., 1995; Rocheleau et al., 1997; Thorpe et al., 1997; Whangbo et al., 2000). Wnts bind to several cell membrane receptors, particularly to a class of seven-transmembrane protein receptors called Frizzled, as well as the Derailed/Ryk receptor tyrosine kinase. Wnt-Frizzled signaling activates diverse downstream pathways, including a "canonical" β-catenin-dependent pathway as well as those independent of β-catenin activation. The latter include pathways that determine planar cell polarity in *Drosophila* or that control vertebrate gastrulation movements (Veeman et al., 2003).

One emerging concept in the axon guidance field is that morphogens that regulate early patterning events are reused later as axon guidance cues (Charron and Tessier-Lavigne, 2005; Schnorrer and Dickson, 2004). Shh, a morphogen that patterns the ventral spinal cord in vertebrates, promotes ventral migration of commissural axons (Charron et al., 2003). The dorsalizing morphogen BMP7 repels the same commissural axons away from the dorsal spinal cord (Butler and Dodd, 2003). Recent evidence suggests that Wnts can also function as axon guidance cues (Liu et al., 2005; Lyuksyutova et al., 2003; Yoshikawa et al., 2003). In *Drosophila*, ectopic expression of the Derailed receptor prevents posterior commissure axons from extending across this commissure (Bonkowsky et al., 1999). This guidance requires Wnt5, suggesting that Wnt5 binds Derailed to repel axons away from the posterior commissure (Yoshikawa et al., 2003). In the mammalian spinal cord, *Wnt4* mRNA is expressed in a rostral-caudal gradient, and ectopic Wnt4 can attract commissural axons that have crossed the midline. Mice lacking the Frizzled receptor Fz3 display A/P axon guidance defects, suggesting that Wnt-Frizzled signaling controls anterior guidance (Lyuksyutova et al., 2003). While an in vivo role for Fz3 in commissural axon guidance has been established, these observations are lacking for the Wnts and other Frizzled receptors. This task is particularly daunting in mammals, in which the number of Wnt and Frizzled genes is high. The mouse genome, for example, encodes 19 Wnts and 12 Frizzled receptors (http://www.stanford.edu/~rnusse/wntwindow.html).

*Correspondence: garriga@berkeley.edu

[5] Present address: Department of Biological Sciences, Lock Haven University of Pennsylvania, Lock Haven, Pennsylvania 17745.

The *C. elegans* genome, by contrast, encodes five Wnts and four Frizzled receptors (http://www.wormbase.org). The relatively small number of Wnts and Frizzleds in *C. elegans* has made it possible to assess their roles, and we find that all five Wnts function in neuronal migration, with significant functional overlap between different paralogs. A subset of these Wnts also controls the anterior guidance of growth cones. Moreover, we provide genetic evidence indicating that at least one of the Wnts functions as a repulsive cue, an effect that is mediated by Frizzled receptors.

Results

C. elegans Wnts and Frizzled Receptors Regulate the Migrations of the HSNs

The *C. elegans* hermaphrodite-specific neurons (HSNs) are a pair of bilaterally symmetric motor neurons that innervate vulval muscles and stimulate hermaphrodites to lay eggs (Desai et al., 1988). They are generated in the tail and migrate anteriorly during embryogenesis (Figure 1A), and their final positions can be easily scored shortly after the completion of their migrations in newly hatched, first larval-stage (L1) hermaphrodites (Figure 1B).

HSN migration requires the Wnt EGL-20 and the Frizzled receptor MIG-1 (see Experimental Procedures for *mig-1* cloning); in *egl-20* and *mig-1* mutants, the HSNs terminate their migrations prematurely and can be found posterior to their normal positions (Desai et al., 1988; Figure 1). *C. elegans* has four additional Wnts (CWN-1, CWN-2, LIN-44, and MOM-2) and three additional Frizzled receptors (CFZ-2, LIN-17, and MOM-5), and we assessed their roles in HSN migration (Figures 1C and 1D; for distributions of the HSNs, see Figure S1 in the Supplemental Data available with this article online). All of the alleles used in this study are considered to be null or strong loss-of-function alleles (see Table S1).

Our phenotypic analysis revealed that all of the Wnt and Frizzled genes are involved in HSN migration. While *cwn-1*, *cwn-2*, *lin-44*, and *mom-2* single mutants had few or no posteriorly displaced HSNs, analysis of double mutants revealed a role in HSN migration for these Wnts. The *lin-44*, *cwn-1*, and *mom-2* mutations all significantly enhanced the HSN migration defects of *egl-20* mutants. More cells were posteriorly displaced (Figure 1C), and they had more severe migration defects (Figure S1). Because mutations in *mom-2* cause a maternal effect, embryonic lethality that precluded us from analyzing HSNs in hermaphrodites lacking both maternal and zygotic MOM-2 function, we analyzed the phenotypes of homozygous mutant hermaphrodites that retain maternal function (*mom-2*(*m+, z−*)). MOM-2 could play a more important role in HSN migration that is masked by the maternal function provided in *mom-2*(*m+, z−*) hermaphrodites. *cwn-2* is tightly linked to *egl-20*, preventing us from easily making the double mutant. Instead, we analyzed *cwn-1; cwn-2* double mutants and found that they had significant HSN migration defects not seen in the single mutants (Figure 1C; Figure S1).

While mutations in the two Frizzled receptor genes *mom-5* and *cfz-2* or the Derailed/Ryk gene *lin-18* had no effect on HSN migration, they enhanced the HSN defects of *mig-1* mutants (Figure 1D; Figure S1). As with *mom-2*, mutations in *mom-5* resulted in a maternal effect, embryonic lethality, raising the possibility that *mom-5* has a more important role in HSN migration. We found that mutations in another Frizzled gene, *lin-17*, suppressed the HSN migration defects of *mig-1* or those of *mig-1; cfz-2* mutants (Figure 1D; Figure S1). We observed the *mig-1* suppression with a second *lin-17* allele (not shown). These observations suggest that LIN-17 can antagonize MIG-1 signaling.

Wnts and Frizzleds Function in A/P Guidance of the AVM and PVM Mechanosensory Neurons

In addition to neuronal cell migrations, we also examined guidance of the processes of two mechanosensory neurons, AVM and PVM. A single process from each neuron extends ventrally, enters the ventral nerve cord, and then turns anteriorly (Figures 2A and 2B). While these growth cones grow ventrally between an epithelium and basement membrane, they extend along an existing axon bundle in the ventral cord. AVM mediates the worm's response to light touch on the anterior body wall, and its process terminates near the tip of the head and branches in the nerve ring, the major *C. elegans* neuropil, where it forms synapses with other neurons. The PVM process terminates in the anterior body region (White et al., 1986).

We used the *Pmec-4::gfp* reporter transgene *zdIs5* to visualize AVM and PVM processes (Figure 2B). Unlike HSN migration, where loss of *egl-20* or *mig-1* had significant effects, none of the Wnt, Frizzled, or *lin-18*/Ryk single mutants exhibited significant AVM or PVM process defects (Figure 2F). Double Wnt *cwn-1; egl-20* and Frizzled receptor *mig-1 mom-5* mutants, by contrast, displayed several types of A/P guidance defects (Figures 2C–2F; for a detailed description, see Table S2). Sometimes the processes stopped prematurely: the AVM process failed to reach the nerve ring, and the PVM process stopped near the midbody (Figure 2C). In other cases, the AVM or PVM process branched in the ventral nerve cord, extending processes both anteriorly and posteriorly (Figure 2D). The most striking phenotype exhibited by the double mutants was when an AVM or PVM process extended to the ventral nerve cord and turned posteriorly toward the tail (Figure 2E). *mig-1; lin-18* mutants had similar PVM, but not AVM, guidance defects (Figure 2F; Table S2). In contrast to the A/P guidance defects, extension to the ventral nerve cord and branching into the nerve ring were largely unaffected in these double mutants, suggesting that these Wnts and Frizzled receptors function specifically in A/P guidance.

Three Wnts, EGL-20, CWN-1, and LIN-44, Are Expressed in the Tail of Embryos and Larvae

We used GFP-translational reporters to study the expression patterns of two Wnt genes, EGL-20 and CWN-1. The integrated array *muIs49* contained a genomic *egl-20* fragment with GFP fused in frame to sequences encoding the C terminus of EGL-20; larvae containing this transgene express GFP in a group of epidermal and muscle cells in the posterior near the anus (Whangbo and Kenyon, 1999). In embryos bearing this transgene, we could not detect GFP fluorescence at the time when the HSNs migrate. We stained *muIs49* embryos with an anti-GFP antiserum and found that these embryos express GFP in several cells of the developing tail beginning just before the comma stage and continuing throughout

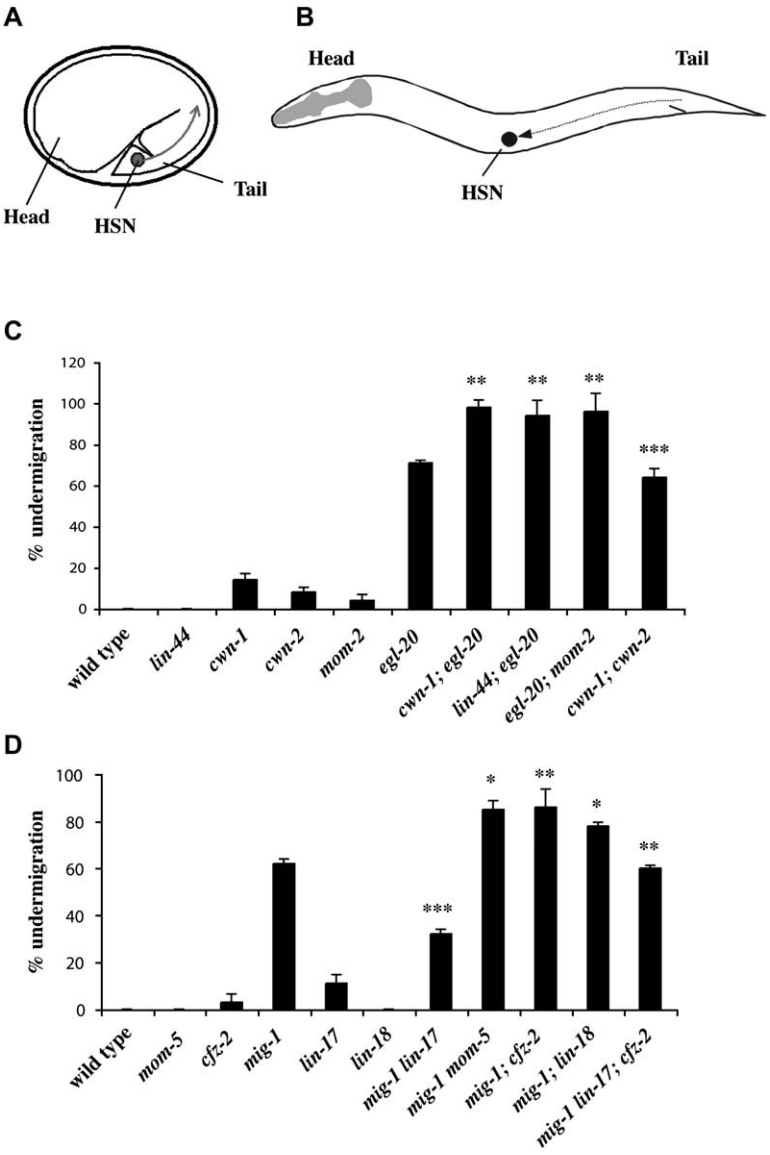

Figure 1. HSN Migration Defects in Wnt and Frizzled Mutants

(A) Schematic diagram of an embryo showing the HSN birthplace and the route of its migration (arrow).

(B) Schematic diagram of a lateral view of a first-stage larva. The arrow indicates the HSN migration route.

(C and D) Graphs showing the percentage of HSNs that failed to migrate to the wild-type position between the P5/6 and V4 hypodermal cells in (C) Wnt and (D) Frizzled mutants, with standard errors. Numbers of HSNs scored for each mutant were: wild-type, 50; *lin-44*, 20; *cwn-1*, 42; *cwn-2*, 25; *mom-2*, 24; *egl-20*, 87; *cwn-1; egl-20*, 59; *lin-44; egl-20*, 33; *egl-20; mom-2*, 29; *cwn-1; cwn-2*, 31; *mom-5*, 18; *cfz-2*, 31; *mig-1*, 89; *lin-17*, 47; *lin-18*, 20; *mig-1 lin-17*, 53; *mig-1 mom-5*, 28; *mig-1; cfz-2*, 47; *mig-1; lin-18*, 60; *mig-1 lin-17; cfz-2*, 47. (C) Mutations in *cwn-1*, *lin-44*, and *mom-2* all significantly enhanced the HSN defects of the *egl-20* mutant (**, $p < 0.01$), and HSN defects of *cwn-1; cwn-2* double mutants were more severe than those in either single mutant (***, $p < 0.0001$). (D) Mutations in the genes *mom-5*, *cfz-2*, and *lin-18* all significantly enhanced the HSN defects of the *mig-1* mutant, while those in *lin-17* significantly suppressed the HSN defects of *mig-1* or *mig-1; cfz-2* mutants (*, $p < 0.05$; **, $p < 0.01$; ***, $p < 0.0001$). The *lin-17* allele in the *mig-1 lin-17* mutant was *n671*, and that in the *mig-1 lin-17; cfz-2* mutant was *n677*. Both are nonsense mutations and are considered to be null.

embryogenesis and larval development (Figures 3A, 3E, and 3I; data not shown). To reveal the relationship between migrating HSNs and EGL-20-expressing cells, we stained embryos carrying both *muIs49* and *muIs13* (*Pegl-5::lacZ*) transgenes with antisera against GFP and LacZ. The Hox gene *egl-5* is expressed in HSNs and a few cells in the tail (Wang et al., 1993) (Figures 3B, 3F, and 3J). We observed that the HSNs migrated away from the EGL-20 source (Figures 3C, 3G, and 3K).

We also generated a *cwn-1::gfp* construct by fusing GFP to genomic sequences encoding CWN-1. This construct was used to generate the extrachromosomal array *gmEx371*. While we were unable to detect GFP fluorescence in embryos or larvae carrying *gmEx371*, we did detect CWN-1::GFP with an anti-GFP antiserum (Figure 3M). The GFP expression was more dynamic than that of EGL-20::GFP. We first detected GFP expression in the embryonic tail beginning at the comma stage. In the newly hatched larvae, CWN-1 was often expressed in four stripes of cells lining the dorsal and ventral posterior quadrants of the body, suggesting that most of the CWN-1-expressing cells were muscle cells (data not shown). The expression spread anteriorly and became more restricted to the ventral side of the animal as development proceeded.

Another Wnt, LIN-44, had also been shown to be expressed in the tail at the time when the HSNs migrate (Herman et al., 1995). Figure 3O illustrates the expression patterns for each of the three Wnts, CWN-1, EGL-20, and LIN-44. The posterior expression of these Wnts raises the interesting possibility that they repel the HSNs and other neurons anteriorly. This hypothesis makes two predictions. First, Wnts should act directly on the HSNs to promote their migrations. Second, ectopic expression of the Wnts should alter HSN migration.

The Frizzled Receptor MIG-1 Functions Cell Autonomously in the Anterior Migrations of the HSN Cell Bodies and the AVM/PVM Growth Cones

To test whether Wnts act directly on the cells that require their function, we asked whether expression of the Frizzled receptor MIG-1 in the HSNs could rescue their

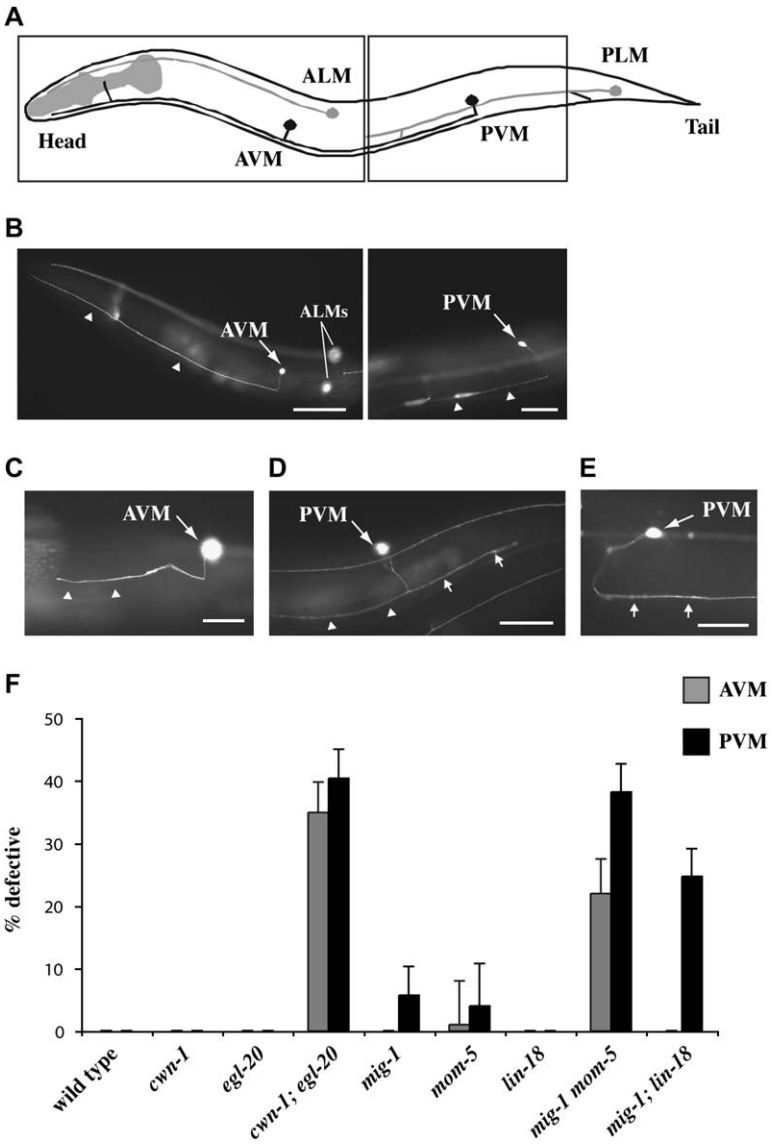

Figure 2. AVM and PVM A/P Guidance Defects in Wnt and Frizzled Mutants

(A) Schematic diagram of the touch neuron ALM, AVM, PVM, and PLM cell bodies and their processes. Only one each of the two bilaterally symmetric ALMs and PLMs are shown. Although both the AVM and PVM neurons are shown, they are on opposite sides of the animal. The boxes represent the portions of the animal shown in (B).

(B–E) Fluorescence photomicrographs of larvae bearing a *Pmec-4::gfp* transgene that expressed GFP in the six touch neurons. (B) The left and right photomicrographs show anterior and posterior midbody views, respectively, of wild-type larvae. Arrowheads mark the AVM (left) and PVM (right) anteriorly directed processes in the ventral nerve cord. (C–E) The three photomicrographs show the three classes of AVM/PVM guidance defects seen in double mutants. (C) The AVM process terminates prematurely along its anterior trajectory (arrowheads). (D) The PVM process branches in the ventral cord, forming an anteriorly directed process (arrowheads) and an abnormal posteriorly directed process (arrows). (E) The PVM process extends posteriorly in the ventral cord (arrows).

(F) The A/P guidance defects of AVM and PVM. The percent defective are all processes displaying one of the three phenotypic classes represented in (C)–(E), with standard errors. Numbers of processes scored for each mutant were (AVM/PVM): wild-type, 106/106; *cwn-1*, 70/70; *egl-20*, 104/104; *cwn-1; egl-20*, 106/109; *mig-1*, 54/54; *mom-5*, 100/101; *lin-18*, 62/62; *mig-1 mom-5*, 100/102; *mig-1; lin-18*, 81/81.

The scale bars = 30 μm.

migration defects in *mig-1* mutants. Many *C. elegans* neuronal lineages express the POU domain protein UNC-86 (Finney and Ruvkun, 1990), and fragments of the *unc-86* gene can drive a more restricted pattern of expression (Baumeister et al., 1996). We generated transgenic animals that used *unc-86* sequences to drive expression of a *mig-1* cDNA fused to GFP (*gmEx384*). In the posterior of the transgenic embryos, only the HSNs and PLM neurons expressed GFP (data not shown). Expression of MIG-1::GFP in the HSNs rescued the HSN migration defects of *mig-1* mutants (Figure 4A), suggesting that MIG-1 functions in the HSNs to promote their migration.

To test whether Wnts act directly on the AVM/PVM neurons, we asked whether expression of MIG-1 in these cells could rescue their A/P guidance defects in *mig-1 mom-5* mutants. The six mechanosensory neurons (2 ALMs, 2 PLMs, AVM, and PVM) express the β-tubulin MEC-7 (Hamelin et al., 1992). We generated transgenic animals that expressed a *mig-1* cDNA fused to GFP from the *mec-7* promoter (*gmEx414*). Expression of MIG-1::GFP in the AVM and PVM of *mig-1 mom-5* mutants significantly rescued their A/P guidance defects (Figure 4B), suggesting that MIG-1 functions in the AVM and PVM to promote the anterior growth of their processes.

EGL-20 Functions as a Repellent for the HSN Migration

To test the hypothesis that Wnts can function as HSN repellents, we expressed EGL-20 ectopically and asked if it altered HSN migration. We first expressed EGL-20 ubiquitously from a heat shock promoter. Embryos just prior to the comma stage were heat shocked at 30ºC for 30 min, shortly before the HSNs are generated. While neither heat shock of wild-type embryos lacking the *Phsp::egl-20* transgene nor a mock heat shock treatment of embryos carrying the transgene had any effect on HSN migration (not shown), heat shock of *Phsp::egl-20* embryos caused both under- and overmigration of the HSNs (Figure 5). The HSNs are serotonergic and can be detected in adult animals with anti-serotonin antisera

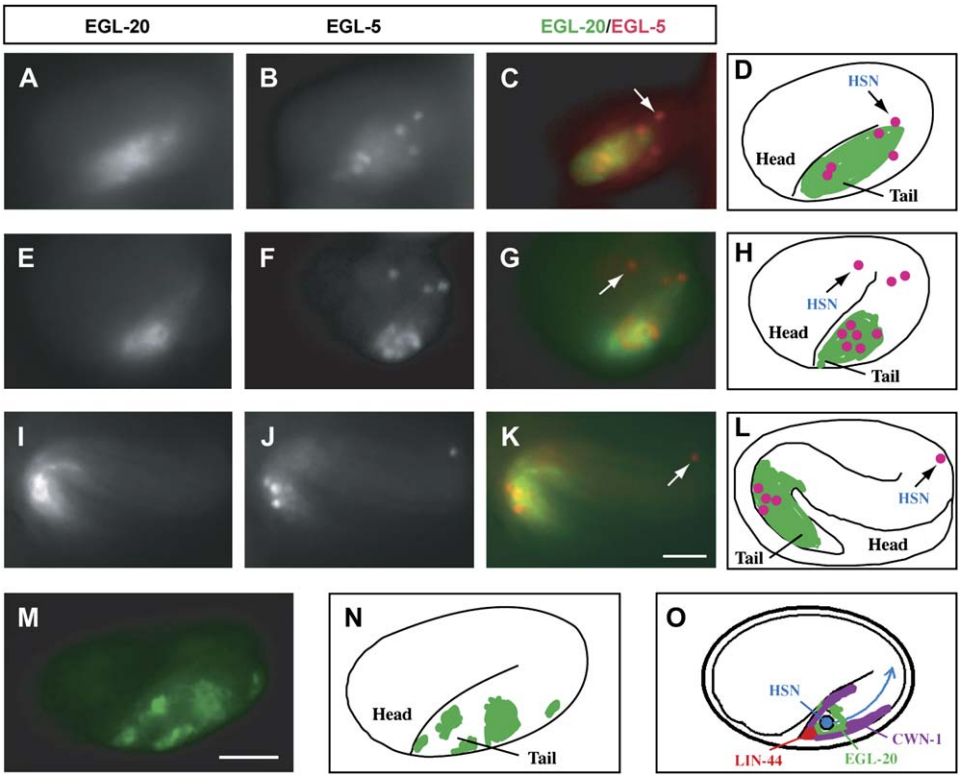

Figure 3. EGL-20 and CWN-1 Are Expressed in the Posterior of the Embryo

(A–O) Fluorescence photomicrographs of embryos bearing the *Pegl-20::egl-20::gfp* transgene *muIs49* and the *Pegl-5::lacZ* transgene *muIs13*. (A, E, I, and M) Anti-GFP staining, (B, F, and J) anti-LacZ staining, and (C, G, and K) anti-GFP and anti-LacZ overlays. Anterior is to the left, and the dorsal side is up. (A–C, E–G, and I–K) HSN nuclei were detected by anti-LacZ staining (arrow), shown in the (A–C) early or (E–G) middle phase of migration, or (I–K) when migration was complete. Only one HSN is in focus. (D, H, and L) Schematic diagrams of (C), (G), and (K), respectively. (M and N) An embryo containing the *Pcwn-1::cwn-1::gfp* extrachromosomal transgenic array *gmEx371*. (O) A schematic diagram of a 1 ½-fold embryo summarizing the expression patterns of CWN-1, EGL-20, and LIN-44. LIN-44 expression at this stage has been previously reported (Herman et al., 1995). The scale bars = 10 μm.

(Desai et al., 1988). All of the HSNs in *Phsp::egl-20* adults that had been heat shocked as embryos could be detected with anti-serotonin antiserum, even the misplaced HSNs, and they expressed normal levels of serotonin, indicating that HSN migration, but not fate, was altered in these animals (data not shown). These results imply that EGL-20 distribution is important for HSN migration.

To elucidate how EGL-20 controls HSN migration, we expressed it from different sites along the A/P axis. If EGL-20 is an HSN repellent, expressing it in the posterior of the embryo should cause the HSNs to migrate too far anteriorly, while expressing it in the anterior should cause the HSNs to terminate their migrations prematurely. One potential problem with the former experiment is that the two canal-associated neurons (CAN), which migrate posteriorly from the head to a location just anterior to the HSNs, can prevent the HSNs from migrating beyond their normal positions (Forrester and Garriga, 1997). To remove this impediment of excessive HSN migration, we conducted our experiments in a *vab-8* mutant background. *vab-8* encodes kinesin-related proteins that are required for posteriorly directed migrations of many neurons and axons, including the migrations of the CANs (Manser and Wood, 1990; Wightman et al., 1996; Wolf et al., 1998). In *vab-8* mutants, the CANs fail to migrate and remain near their birthplace in the head, and the HSNs migrate beyond their normal destinations 31% of the time (Figure 5B).

We first increased the level of endogenous EGL-20 by using the integrated array *muIs49*, which contains extra copies of the *egl-20* gene. While this transgene had no effect on wild-type HSNs (not shown), it enhanced the HSN overmigration phenotype of *vab-8* mutants (Figure 5B). We next moved the expression domain of EGL-20 forward. Several cells in the posterior midbody region express the Hox gene *mab-5* (Cowing and Kenyon, 1992; Salser and Kenyon, 1992). This expression overlaps with and extends anteriorly from the domain of *egl-20* expression. While expression of an *egl-20* cDNA from the *mab-5* promoter had no effect on wild-type HSNs (not shown), it enhanced the HSN overmigration phenotype of *vab-8* mutants (Figure 5B). Moreover, we observed that in *vab-8* animals carrying this transgene, the HSNs migrated farther than those in the *vab-8; muIs49* animals (Figure 5B).

We next tested whether expressing EGL-20 in the head would prevent the HSNs from migrating too far anteriorly in a *vab-8* mutant. The gene *lim-4* is expressed in the AWB, SAA, SIA, RIV, RID, RMEV, and two of the six RMD neurons in larvae and adult animals (Sagasti et al., 1999). We found that *lim-4* was also expressed in several cells in the head of embryos (not shown). While

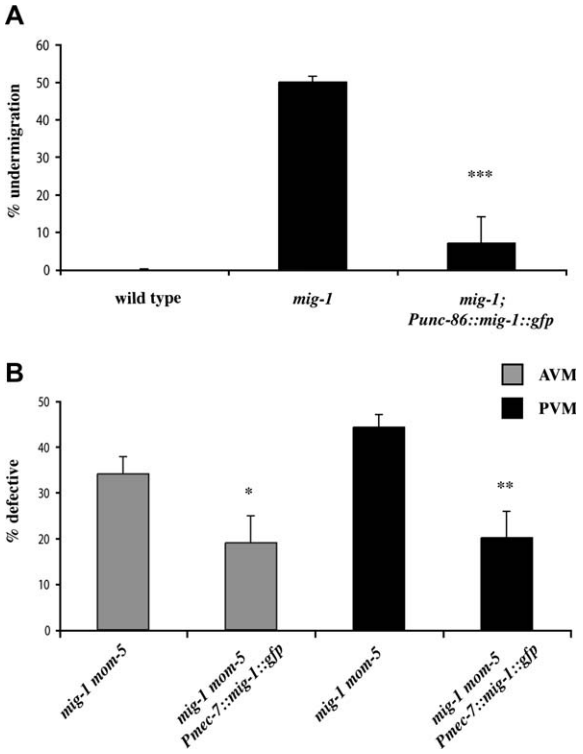

Figure 4. MIG-1 Functions Cell Autonomously to Promote HSN Migration and the Guidance of AVM and PVM Processes

(A) Expression of MIG-1::GFP in the HSNs rescues the HSN migration defect of *mig-1*(*e1787*) mutants. The *mig-1* animals that had the array *gmEx384*(*Punc-86::mig-1::gfp*) or their siblings that had lost the array (*mig-1*) were raised at 25ºC. Numbers of animals scored are: *mig-1*, 68; *mig-1; gmEx384*, 113 (***, $p < 0.0001$).

(B) Expression of MIG-1::GFP in the AVM/PVM rescues the migration defects of their growth cones in the *mig-1*(*e1787*) *mom-5* (*ne12*) mutants. The classification of defects is the same as that in Figure 2F. The *mig-1 mom-5* animals that had the array *gmEx414* (*Pmec-7::mig-1::gfp*) or their siblings that had lost the array (*mig-1 mom-5*) were raised at 25ºC. Numbers of processes scored are: AVM, *mig-1 mom-5*, 82; *mig-1 mom-5; gmEx414*, 105; PVM, *mig-1 mom-5*, 79; *mig-1 mom-5; gmEx414*, 104 (*, $p < 0.05$; **, $p < 0.001$). Bars indicate standard errors.

expression of an *egl-20* cDNA from the *lim-4* promoter had no effect on wild-type HSNs, it reduced the HSN overmigration phenotype of *vab-8* mutants (Figure 5B).

To rule out the possibility that these effects were dependent on the *vab-8* mutant background, we also placed the *Pmab-5::egl-20::gfp* and *Plim-4::egl-20::gfp* transgenes in a *ceh-10(gm58)* mutant background. CEH-10 is a homeodomain protein that specifies the fates of several neurons, including the CANs (Altun-Gultekin et al., 2001; Forrester et al., 1998). The CANs fail to differentiate and migrate in *ced-10(gm58)* mutants, but unlike *vab-8* mutants, other migrations are largely unaffected. As in *vab-8* mutants, the HSNs migrated too far anteriorly in *ceh-10* mutants 30% of the time (n = 100), and the effects of the transgenes on HSN migration were similar. Expression of *egl-20* from the *mab-5* promoter significantly increased the frequency of these anterior HSNs to 62% (n = 60; $p < 0.0001$), and expression from the *lim-4* promoter decreased the frequency to 17% (n = 76; $p < 0.05$). Taken together with the results from the MIG-1 cell autonomy experiments, these results indicate that EGL-20 can function as an HSN repellent.

EGL-20 Functions as a Repellent through the Frizzled Receptors MIG-1 and MOM-5 to Control the A/P Guidance of the AVM and PVM Processes

Posterior expression of EGL-20 and CWN-1 and the requirement of these two Wnts for the anteriorly directed extensions of AVM and PVM processes also raised the possibility that Wnts can function as repulsive cues for growth cones. While neither the *Pmab-5::egl-20::gfp* transgene nor the *Plim-4::egl-20::gfp* transgene had an effect on the ability of the AVM or PVM processes to extend to the head (data not shown), we noticed that the AVM and ALM branches failed to extend normally into the nerve ring in *Plim-4::egl-20::gfp* animals. In wild-type animals, the AVM and the two ALM branches enter the nerve ring ventrally and dorsally, respectively, and form gap junctions where they meet (White et al., 1986). Visualization of the ALM and AVM branches with the *Pmec-4::gfp* transgene shows that they encircle the nerve ring (Figures 6A and 6B). Expression of *egl-20* from the *lim-4* promoter revealed EGL-20::GFP expression in several neurons near the nerve ring (see above), many of which contribute axons to the nerve ring (Sagasti et al., 1999). This ectopic expression disrupted ALM and AVM branching into the nerve ring (Figures 6C and 6D). These branches either stopped short with an engorged end or turned away from the EGL-20-expressing cells. The branching defects occurred at similar frequencies either in wild-type or in Wnt mutant backgrounds (Figure 6D and data not shown). The finding that the ALM branches were also affected in this experiment was not surprising. CWN-1, CWN-2, and EGL-20 act in ALM guidance: the anterior ALM processes were rerouted posteriorly in *cwn-1; egl-20* and *cwn-1; cwn-2* Wnt double mutants (Hilliard and Bargmann, 2006 [this issue of *Developmental Cell*]; B. Prasad and S.G. Clark, submitted; C.-L.P. and G.G., unpublished data).

The ALM and AVM branching defects in *Plim-4::egl-20::gfp* transgenic animals suggests that EGL-20 could act as a repellent to guide these processes forward. To test this hypothesis, we first expressed EGL-20 broadly by using a heat shock promoter. Heat shock of these transgenic animals resulted in posterior rerouting of both the AVM and PVM processes, consistent with EGL-20's distribution being important for guidance (Figure 7A). To test the hypothesis further, we asked whether ectopic expression of EGL-20 in the anterior or posterior could have an effect in the double Wnt mutant *cwn-1; egl-20*, where AVM and PVM guidance in the ventral nerve cord is perturbed. Expression of *egl-20* from the *mab-5* promoter in a domain that is posterior to the AVM and PVM neurons almost completely rescued the AVM guidance defects and partially rescued the PVM defects (Figure 7A). Expression of *egl-20* from the *lim-4* promoter in several neurons in the head enhanced the AVM/PVM guidance defects of the double mutants (Figure 7A). These results suggest that EGL-20 normally functions as a repellent for the anterior guidance of the AVM and PVM processes.

Since the *mig-1 mom-5* double Frizzled mutants had similar guidance defects as the *cwn-1; egl-20* double

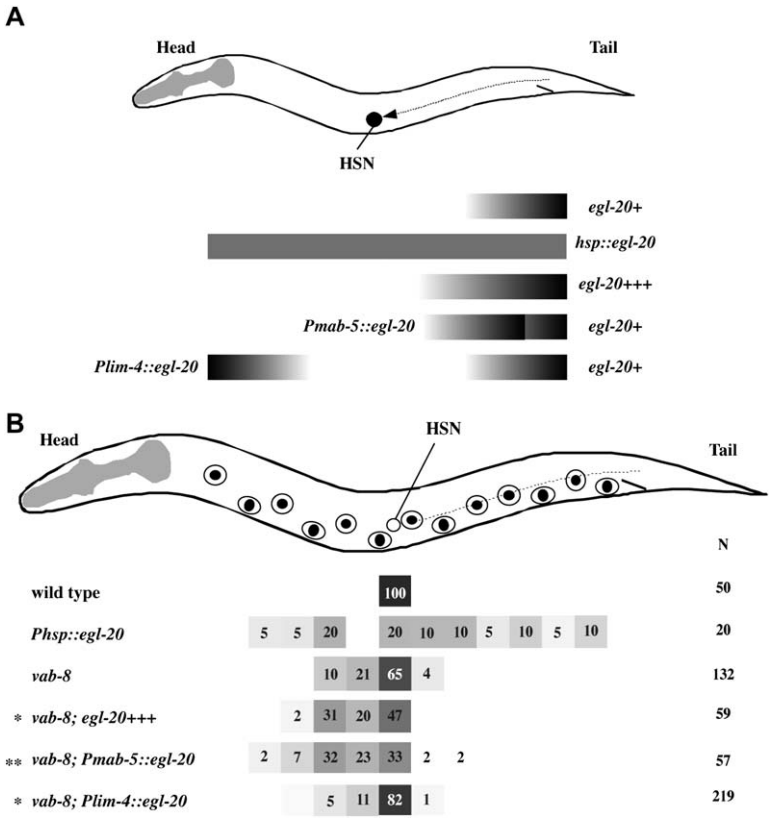

Figure 5. EGL-20 Is an HSN Repellent

(A) Schematic diagram showing the predicted EGL-20 distributions in wild-type and transgenic hermaphrodites.

(B) Graph representing the distributions of the HSNs in wild-type and transgenic hermaphrodites. The open circles and ovals represent the positions of the V and P cell nuclei, respectively. The filled circles represent nucleoli of V and P cells. In wild-type hermaphrodites, the HSNs migrate to positions between the P5/6 and V4 hypodermal cells. Those HSNs found anterior to P5/6 were scored as overmigrated; those HSNs found posterior to V4 were scored as undermigrated. In *vab-8* animals, 31% HSNs migrated anterior to their normal destination. The integrated *Pegl-20::egl-20::gfp* array *muIs49* and the extrachromosomal *Pmab-5::egl-20::gfp* array *gmEx317* enhanced the HSN overmigration of the *vab-8* mutants. *vab-8*-dependent HSN overmigration was significantly reduced by the *Plim-4::egl-20::gfp* array *gmEx365* (*, $p < 0.005$; **, $p < 0.0001$).

Wnt mutants, we tested whether MIG-1 and MOM-5 mediate EGL-20's effects. If EGL-20 acts though MIG-1 and MOM-5, ectopic expression of EGL-20 in a *mig-1 mom-5* mutant background should no longer affect A/P guidance of the AVM and PVM growth cones. Consistent with this model, we found that the ectopic expression of EGL-20 did not affect most of the guidance defects of the *mig-1 mom-5* mutants (Figure 7B). In contrast to the effects of ectopic EGL-20 expression on the AVM/PVM processes of *cwn-1; egl-20* mutants, the *Pmab-5::egl-20::gfp* transgene failed to rescue the AVM/PVM defects of *mig-1 mom-5* mutants, and the *Plim-4::egl-20::gfp* transgene did not enhance the PVM defects of the double mutant (Figure 7B). We did observe that the *Plim-4::egl-20::gfp* transgene still significantly enhanced the AVM defects of *mig-1 mom-5* mutants, suggesting that while EGL-20 guides the AVM/PVM growth cones by acting through MIG-1 and MOM-5, EGL-20 might act through receptors other than these two Frizzled molecules in AVM guidance.

We also found that the branching defects caused by the *Plim-4::egl-20::gfp* transgene were partially suppressed in *mig-1 mom-5* mutants (Figure 6D). The frequency of branching defects in the *mig-1 mom-5* double mutants, however, was still higher when ectopic EGL-20 was present, indicating that some EGL-20 signal is received in the double mutant. This effect could be mediated by another receptor or by maternally provided *mom-5*. Together, our results indicate that EGL-20 functions as a repellent, and that it acts through the two Frizzled receptors MIG-1 and MOM-5 to control A/P guidance of the AVM and PVM processes.

Discussion

Functional Redundancy and Specificity of Wnt Proteins

Both Wnts and Frizzled receptors are encoded by multiple genes. The mouse and human genomes encode 19 Wnts, and 10 and 12 Frizzled receptors, respectively. *C. elegans* has five Wnts and four Frizzled receptors, making a complete genetic analysis of their roles in development feasible. This relative simplicity has led to an understanding of how multiple Wnts and their receptors regulate vulval development in *C. elegans* (Inoue et al., 2004). Our phenotypic analysis of Wnt and Frizzled mutants reveals that multiple Wnts and Frizzled receptors function in cell and growth cone migrations. While only loss of EGL-20/Wnt or MIG-1/Frizzled resulted in significant HSN migration defects, loss of the remaining Wnt and Frizzled receptors altered HSN migration in *egl-20* or *mig-1* mutant backgrounds. Supporting the hypothesis that different Wnts provide overlapping functions, we found that excess EGL-20 rescued the migration defects of the QR neuroblast caused by the *cwn-1* mutation (data not shown). However, we also observed that *lin-44* mutations could enhance the HSN migration defects of *egl-20*, but not *cwn-1*, mutants (data not shown), suggesting that not all of the Wnts function in the same way to promote HSN migration.

Several models can account for the overlapping roles of the different Wnts in neuronal cell body and growth cone migrations. First, different Wnt proteins could form heterodimers with more activity than individual homodimers. Two members of the BMP family, GDF7 and

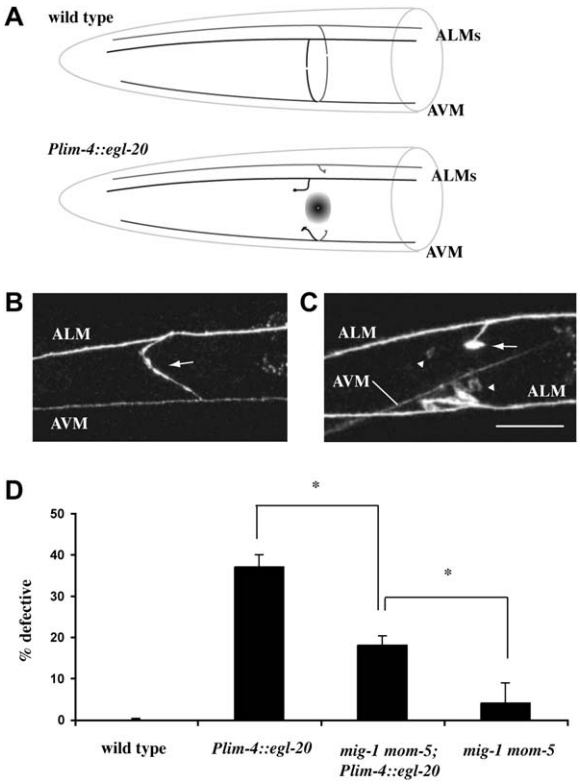

Figure 6. EGL-20 Repels the ALM and AVM Nerve Ring Branches

(A) Schematic diagram of the ALM and AVM nerve ring branches in wild-type and *gmEx365*(*Plim-4::egl-20::gfp*) transgenic animals.

(B) Confocal image of the nerve ring in a wild-type animal carrying a *Pmec-4::gfp* reporter, which expresses GFP in the ALM and AVM processes.

(C) Confocal image of the nerve ring in a wild-type animal carrying a *Pmec-4::gfp* reporter and a *Plim-4::egl-20::gfp* transgenic array. Several neurons in the head ganglia express EGL-20::GFP (arrowheads). The ALM and AVM branches stop prematurely (arrow) or seemed to be repelled away from the EGL-20-expressing cells. Animals bearing *gmEx365* are rollers, and the oblique line in (C) is the AVM process as indicated. The scale bar = 30 μm.

(D) Percentage of the nerve ring defects in animals carrying the *Plim-4::egl-20::gfp* transgenic array, with standard errors. Animals with the array had nerve ring defects that their siblings without the array lacked, and this effect is similar in either wild-type or various Wnt mutant backgrounds (data not shown). Numbers of animals scored are: wild-type, 106; *gmEx365*, 73; *mig-1 mom-5*, 55; *mig-1 mom-5; gmEx365*, 38. In mutant backgrounds where the AVM process may fail to project to the nerve ring, we scored only AVM processs that reached the nerve ring and hence were able to project a branch into the nerve ring. The *mig-1 mom-5; gmEx365* animals had less nerve ring defects compared to *gmEx365* animals, indicating that MIG-1 and MOM-5 are required for the repulsive effects of EGL-20 on the nerve ring branches (*, $p < 0.05$).

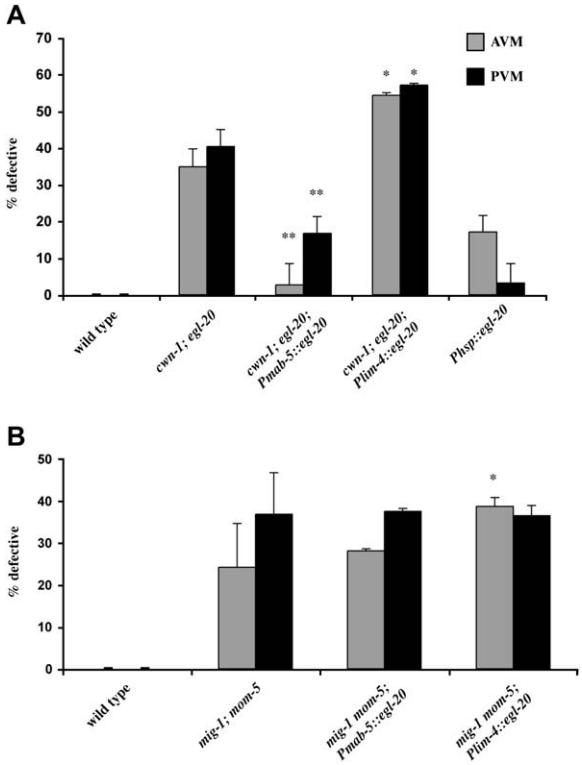

Figure 7. EGL-20 Is a Repellent for the Anterior Guidance of AVM and PVM Processes

(A) The predicted EGL-20 distributions in the transgenic animals used for this figure are shown in Figure 5A. In *cwn-1; egl-20* animals, 35% of the AVM and 40% of the PVM processes scored had defective A/P guidance (n = 106 and 109, respectively). Heat shock of *Phsp::egl-20* L1 larvae caused A/P guidance defects of AVM/PVM processes (17.1% defective for AVM processes, 70 animals; and 3.2% defective for PVM processes, 63 animals). For the heat-shocked animals, only branching and posterior rerouting defects of the adult animals were scored. The extrachromosomal *Pmab-5::egl-20::gfp* array *gmEx317* significantly rescued these defects (3% of AVM and 17% of PVM processes were defective, n = 73 and 72, respectively; **, $p < 0.0001$). By contrast, the A/P guidance defects were significantly enhanced by the *Plim-4::egl-20::gfp* array *gmEx365* (54% of AVMs and 58% of PVMs, n = 103 and 105, respectively; *, $p < 0.05$).

(B) MIG-1 and MOM-5 are receptors for EGL-20 in the anterior guidance of AVM and PVM processes. The defects in *mig-1 mom-5* mutants are comparable to those of the *cwm-1; egl-20* mutants (24% of AVMs and 37% of PVMs defective, n = 264 and 266, respectively). Neither *gmEx317* nor *gmEx365* had a significant effect on the severity of PVM guidance defects in the *mig-1 mom-5* mutants. However, we did observe a significant effect of *gmEx365* on the AVM guidance of the *mig-1 mom-5* mutant (numbers of AVM/PVM processes scored, *mig-1 mom-5; gmEx317*, 32/32; *mig-1 mom-5; gmEx365*, 63/64; *, $p < 0.05$).

Bars indicate standard errors.

BMP7, form heterodimers with stronger axon repulsive activity than the BMP7 homodimer (Butler and Dodd, 2003). While Wnt dimers have not been observed, Frizzled dimerization may be important for signaling (Carron et al., 2003). Second, CWN-1, CWN-2, LIN-44, and MOM-2 may promiscuously bind the same Frizzled receptors as EGL-20. Wnts are known to interact with multiple Frizzled receptors (Wu and Nusse, 2002). Finally, different Wnts may participate in somewhat independent, parallel pathways to control migration. EGL-20, for example, could act as a guidance cue, and one of the other Wnts could regulate the transcription of genes involved in anteriorly directed migrations. Differences in the concentrations of Wnts or in their affinity for Frizzled receptors may also determine the specificity of signaling pathways (Rulifson et al., 2000). A challenge in the future will be to determine whether all of the Wnts act as guidance cues or possess distinct functions in cell migration and axon guidance and to define which Frizzled receptors mediate the effects of the different Wnts.

Wnt Signaling Regulates Cell Migration and Axon Guidance though Distinct Mechanisms

In *C. elegans*, Wnt signaling had been shown to control neuronal migrations (Maloof et al., 1999). In our study and two separate studies (Hilliard and Bargmann, 2006; B. Prasad and S.G. Clark, submitted), Wnt signaling was found to control the migration of growth cones. The fascinating revelation from these different studies is that Wnt signaling acts by distinct mechanisms to regulate cell and growth cone migrations along the *C. elegans* A/P axis. EGL-20/Wnt causes the QL neuroblast and its descendents to migrate posteriorly (Maloof et al., 1999; Whangbo and Kenyon, 1999). Acting through a β-catenin canonical pathway, EGL-20/Wnt transcriptionally activates the Hox gene *mab-5* in QL and its descendents; acting through unidentified target genes, MAB-5 causes these cells to migrate posteriorly (Korswagen et al., 2002; Maloof et al., 1999; Whangbo and Kenyon, 1999). The distribution of EGL-20 is not important for its role in QL migration, as different A/P sources of EGL-20 can rescue the QL phenotype of *egl-20* mutants (Whangbo and Kenyon, 1999). LIN-44/Wnt and LIN-17/Frizzled determine the polarity of process outgrowth from the mechanosensory neuron PLM (Hilliard and Bargmann, 2006; B. Prasad and S.G. Clark, submitted). The PLM neurons extend a short posterior process and a long anterior process. In *lin-44* and *lin-17* mutants, the polarity of the PLM neuron is reversed. Hilliard and Bargmann (2006) have found that, as with the control of QL migration, the distribution of this Wnt does not appear to be essential for its function, since ubiquitously expressed LIN-44 can partly rescue the PLM polarity defects.

The posterior expression of the three Wnts EGL-20, CWN-1, and LIN-44 prompted us to test the possibility that Wnts may function as repulsive cues for neurons and growth cones that migrate anteriorly. In contrast to the role of Wnts in QL neuroblast migration and PLM polarity, where their distribution isn't important, EGL-20 acts as a repellent for the migration of the HSNs and AVM/PVM growth cones.

A Conserved Role for Wnts as A/P Guidance Cues?

Taken together with our work, the fly and mammalian studies indicate that Wnts are conserved cues that guide axons along the A/P axis. In *Drosophila*, the growth cones of neurons that express the Ryk receptor Derailed are repelled from the posterior commissure by Wnt5, and instead extend across the midline via the anterior commisssure (Callahan et al., 1995; Yoshikawa et al., 2003). Mammalian Ryk appears to act as a Frizzled coreceptor necessary for neurite outgrowth induced by Wnt3a (Lu et al., 2004) and mediates the ability of Wnts to repel corticospinal tract axons (Liu et al., 2005). The observations that Fz3 is required for commissural axons to extend anteriorly up a Wnt gradient and that Ryk mediates the repulsion from Wnts in mammals and flies have led to the model in which the response to Wnts is mediated by the type of receptor expressed: Frizzled receptors mediate attraction to Wnts, and Ryk mediates repulsion from Wnts (Liu et al., 2005). Our findings are inconsistent with this attractive model. We show that the Frizzled receptors MIG-1 and MOM-5 mediate the repulsive effects of EGL-20, and we found that the *C. elegans* sole Ryk receptor LIN-18 is likely to play a redundant role with MIG-1 in repelling the HSNs and the AVM/PVM growth cones.

While both EGL-20 and mammalian Wnts promote anterior migrations in nematodes and mammals, respectively, they carry out these functions in different ways. Wnt4A is expressed in a decreasing anterior to posterior gradient in the mammalian spinal cord, whereas expression of CWN-1, EGL-20, and LIN-44 in the tail suggests that an opposite Wnt gradient exists in *C. elegans*. Mammalian Wnt4A attracts growth cones though Frizzled3 receptor, *Drosophila* and mammalian Wnts repel growth cones through Ryk receptors, and the *C. elegans* Wnt EGL-20 repels growth cones through Frizzled receptors and possibly through the Ryk LIN-18 receptor. These differences lead us to propose that, while the role of Wnts as guidance cues is conserved among metazoans, how signaling downstream from Wnt receptors is regulated may vary in interesting ways.

Experimental Procedures

Nematode Strains and Genetics

Strains were maintained at 20°C as described (Brenner, 1974). Table S1 describes the alleles used in this study.

mig-1 Cloning

We noticed that the available mapping data for *mig-1* placed it in an interval that contained the gene *cfz-1*, which encodes a predicted Frizzled receptor (Wang et al., 1996). Because it was known at the time that mutations in *mig-1* and the *dsh* gene *mig-5* had similar phenotypes (E. Hedgecock, personal communication), we tested the hypothesis that *mig-1* and *cfz-1* were the same gene by sequencing the *cfz-1* gene from *mig-1* mutants. The *e1787* allele is a Q277 ochre stop (transcript A) or a Q281 ochre stop (transcript B), and the *n687* mutation is a Q150 ochre stop.

Transgenic Animals

The following transgenic strains were used in this study: *zdIs5*(*mec-4::gfp*, *lin-15*[+]); *muIs49*(*Pegl-20::egl-20::gfp*, *unc-22* antisense); *muIs53*(*Phsp16-2::egl-20*, *unc-22* antisense); *gmEx317*(*Pmab-5::egl-20::gfp* [50 ng/μl], *myo-2::gfp* [50 ng/μl]); *gmEx365*(*Plim-4::egl-20::gfp* [100 ng/μl], *rol-6*[*su1006*]); *gmEx371*(*cwn-1::gfp* [100 ng/μl], *rol-6*[*su1006*]); *gmEx384*(*unc-86::mig-1::gfp* [0.5 ng/μl], *dpy-30::NLS::DsRed* [50 ng/μl]); *gmEx414*(*mec-7::mig-1::gfp* [1 ng/μl], *rol-6*[*su1006*]).

Molecular Biology and Germline Transformation

Standard molecular biology techniques were used to construct transgenes. An *egl-20* cDNA was obtained by PCR with pJW27 (J. Withee, personal communication) as a template, with the forward primer 5′-TTTTTTTTCCCGGGATGCAATTTTTCATTTGCCTG-3′ and the reverse primer 5′-TTTTTTTCCCGGGCCTTTGCATGTATGTACTG CA-3′ both containing a SmaI site. The *egl-20* cDNA was then subcloned into GFP vectors containing the promoter sequences of *mab-5* and *lim-4*. To construct *Punc-86::mig-1::gfp*, a 5.1 kb fragment of the sequence upstream of the *unc-86* corresponding to nucleotides 8,216,213–8,221,314 (WormBase: http://www.wormbase.org) was isolated by PCR from genomic DNA with the forward primer 5′-GTTC CCGCATGCACTAGTTTCTAG-3′ (introducing a SphI site) and the reverse primer 5′-GGTGTTGTCGACGTCCGTG-3′ (introducing a SalI site). This *unc-86* promoter sequence was subcloned into pPD95.77 (obtained as a gift from Andrew Fire). Transgenic animals injected with the resulting plasmid recapitulated the reported GFP expression pattern in HSN, Q neuroblast, and other cells (data not shown). A full-length *mig-1* cDNA was amplified by PCR with primers 5′-ATGGGACCATTTCGTG-3′ and 5′-TCAAATCATATTATTAGTTC GA-3′ from a reverse transcriptase (RT) cDNA pool kindly provided by Lianna Wong. We first cloned the *mig-1* cDNA into pPD95.77, and then we cloned the aforementioned *unc-86* promoter sequence into the resulting plasmid. To constuct *mec-7::mig-1*, the *mec-7*

promoter sequence in the Fire vector pPD96.41 was first cloned into the vector pPD95.77. The *mig-1* cDNA was then PCR amplified from a RT-cDNA pool with the primers 5′-AAATGGCCAATGGGACCATTT CGTGGTTAAC-3′ (introducing a MscI site) and 5′-TTTACCGGTAT CATATTATTAGTTCGAAACGTC-3′ (introducing an AgeI site) and fused in frame to the GFP sequence in the vector containing the *mec-7* promoter. Germline transformation was performed by direct injection of various plasmid DNAs into the gonads of adult wild-type animals as described (Mello et al., 1991).

Nomarski Microscopy for HSN Migration

HSN positions were scored in newly hatched L1 hermaphrodites. Their positions were scored relative to the invariant positions of the nonmigrating hypodermal nuclei. HSNs that had failed to migrate anteriorly past P11/12 out of the tail or that had migrated more anteriorly past V1 into the head cannot be unambiguously identified, as they could not be distinguished from other neurons in the tail or head. In strains in which the HSNs failed to migrate fully, if the HSN could not be found, we scored it as having failed to migrate from its birthplace in the tail. In strains in which the HSNs migrated excessively, if the HSN could not be found, we scored it as having migrated anterior to V1.

Immunofluorescence Microscopy

Anti-serotonin staining was performed as described previously (Garriga et al., 1993). Embryos were then fixed and treated as described (Finney and Ruvkun, 1990). Primary antibodies were 1% rabbit anti-serotonin antiserum (1:100, provided by J. Steinbusch, Free University, Amsterdam, The Netherlands), rabbit polyclonal anti-GFP antibody (1:1000, Molecular Probes), or mouse monoclonal anti-LacZ antibody (1:1000, Molecular Probes). Secondary antibodies included 1% Cy3-conjugated donkey anti-rabbit antibody for the anti-serotonin staining (Jackson ImmunoResearch Laboratories), 1% Alexa488-conjugated goat anti-rabbit antibody for the GFP staining, and 1% Alexa-568-conjugated goat anti-mouse antibody for the LacZ staining (Molecular Probes). Images were acquired under the Zeiss Axioskop2 microscope or the Leica TCS NT confocal microscope system.

Supplemental Data

Supplemental Data including the mutant allele information, the distribution of HSN cell bodies in wild-type and mutant animals, and the types of AVM and PVM process defects in different mutant strains are available at http://www.developmentalcell.com/cgi/content/full/10/3/367/DC1/.

Acknowledgments

We thank Cynthia Kenyon for the *muIs49* and *muIs53* transgenes, Andy Fire and Tinya Fleming for various GFP plasmids, Lianna Wong for the mixed N2 cDNA pool, Zemer Gitai for *unc-86* promoter sequence information, Barbara Meyer for the use of the confocal microscope, and the *C. elegans* Genetics Center and the *C. elegans* Knockout Consortium for some of the strains used in this study. This work was supported by National Institutes of Health (NIH) grant NS32057 (G.G.) and by the Howard Hughes Medical Institute (C.I.B.). C.I.B. is an investigator with the Howard Hughes Medical Institute. C.-L.P was supported by a Fellowship for Graduate Study from the Ministry of Education, Taiwan, and S.G.C. was supported by a fellowship from the Helen Hay Whitney Foundation. M.A.H. was supported by a European Molecular Biology Organization Long Term Fellowship.

Received: September 28, 2005
Revised: January 31, 2006
Accepted: February 16, 2006
Published online: March 6, 2006

References

Altun-Gultekin, Z., Andachi, Y., Tsalik, E.L., Pilgrim, D., Kohara, Y., and Hobert, O. (2001). A regulatory cascade of three homeobox genes, *ceh-10, ttx-3* and *ceh-23*, controls cell fate specification of a defined interneuron class in *C. elegans*. Development *128*, 1951–1969.

Baumeister, R., Liu, Y., and Ruvkun, G. (1996). Lineage-specific regulators couple cell lineage asymmetry to the transcription of the *Caenorhabditis elegans* POU gene *unc-86* during neurogenesis. Genes Dev. *10*, 1395–1410.

Bonkowsky, J.L., Yoshikawa, S., O'Keefe, D.D., Scully, A.L., and Thomas, J.B. (1999). Axon routing across the midline controlled by the *Drosophila* Derailed receptor. Nature *402*, 540–544.

Brenner, S. (1974). The genetics of *Caenorhabditis elegans*. Genetics *77*, 71–94.

Butler, S.J., and Dodd, J. (2003). A role for BMP heterodimers in roof plate-mediated repulsion of commissural axons. Neuron *38*, 389–401.

Callahan, C.A., Muralidhar, M.G., Lundgren, S.E., Scully, A.L., and Thomas, J.B. (1995). Control of neuronal pathway selection by a *Drosophila* receptor protein-tyrosine kinase family member. Nature *376*, 171–174.

Carron, C., Pascal, A., Djiane, A., Boucaut, J.C., Shi, D.L., and Umbhauer, M. (2003). Frizzled receptor dimerization is sufficient to activate the Wnt/beta-catenin pathway. J. Cell Sci. *116*, 2541–2550.

Chan, S.S., Zheng, H., Su, M.W., Wilk, R., Killeen, M.T., Hedgecock, E.M., and Culotti, J.G. (1996). UNC-40, a *C. elegans* homolog of DCC (Deleted in Colorectal Cancer), is required in motile cells responding to UNC-6 netrin cues. Cell *87*, 187–195.

Charron, F., and Tessier-Lavigne, M. (2005). Novel brain wiring functions for classical morphogens: a role as graded positional cues in axon guidance. Development *132*, 2251–2262.

Charron, F., Stein, E., Jeong, J., McMahon, A.P., and Tessier-Lavigne, M. (2003). The morphogen sonic hedgehog is an axonal chemoattractant that collaborates with netrin-1 in midline axon guidance. Cell *113*, 11–23.

Cowing, D.W., and Kenyon, C. (1992). Expression of the homeotic gene *mab-5* during *Caenorhabditis elegans* embryogenesis. Development *116*, 481–490.

Desai, C., Garriga, G., McIntire, S.L., and Horvitz, H.R. (1988). A genetic pathway for the development of the *Caenorhabditis elegans* HSN motor neurons. Nature *336*, 638–646.

Dickson, B.J. (2002). Molecular mechanisms of axon guidance. Science *298*, 1959–1964.

Finney, M., and Ruvkun, G. (1990). The *unc-86* gene product couples cell lineage and cell identity in *C. elegans*. Cell *63*, 895–905.

Forrester, W.C., and Garriga, G. (1997). Genes necessary for *C. elegans* cell and growth cone migrations. Development *124*, 1831–1843.

Forrester, W.C., Perens, E., Zallen, J.A., and Garriga, G. (1998). Identification of *Caenorhabditis elegans* genes required for neuronal differentiation and migration. Genetics *148*, 151–165.

Garriga, G., Desai, C., and Horvitz, H.R. (1993). Cell interactions control the direction of outgrowth, branching and fasciculation of the HSN axons of *Caenorhabditis elegans*. Development *117*, 1071–1087.

Hamelin, M., Scott, I.M., Way, J.C., and Culotti, J.G. (1992). The *mec-7* β-tubulin gene of *Caenorhabditis elegans* is expressed primarily in the touch receptor neurons. EMBO J. *11*, 2885–2893.

Herman, M.A., Vassilieva, L.L., Horvitz, H.R., Shaw, J.E., and Herman, R.K. (1995). The *C. elegans* gene *lin-44*, which controls the polarity of certain asymmetric cell divisions, encodes a Wnt protein and acts cell nonautonomously. Cell *83*, 101–110.

Hilliard, M.A., and Bargmann, C.I. (2006). Wnt signals and Frizzled activity orient anterior-posterior axon outgrowth in *C. elegans*. Dev. Cell *10*, this issue, 379–390.

Inoue, T., Oz, H.S., Wiland, D., Gharib, S., Deshpande, R., Hill, R.J., Katz, W.S., and Sternberg, P.W. (2004). *C. elegans* LIN-18 is a Ryk ortholog and functions in parallel to LIN-17/Frizzled in Wnt signaling. Cell *118*, 795–806.

Keino-Masu, K., Masu, M., Hinck, L., Leonardo, E.D., Chan, S.S., Culotti, J.G., and Tessier-Lavigne, M. (1996). Deleted in Colorectal Cancer (DCC) encodes a netrin receptor. Cell *87*, 175–185.

Kennedy, T.E., Serafini, T., de la Torre, J.R., and Tessier-Lavigne, M. (1994). Netrins are diffusible chemotropic factors for commissural axons in the embryonic spinal cord. Cell *78*, 425–435.

Kolodziej, P.A., Timpe, L.C., Mitchell, K.J., Fried, S.R., Goodman, C.S., Jan, L.Y., and Jan, Y.N. (1996). frazzled encodes a *Drosophila* member of the DCC immunoglobulin subfamily and is required for CNS and motor axon guidance. Cell *87*, 197–204.

Korswagen, H.C., Coudreuse, D.Y., Betist, M.C., van de Water, S., Zivkovic, D., and Clevers, H.C. (2002). The Axin-like protein PRY-1 is a negative regulator of a canonical Wnt pathway in *C. elegans*. Genes Dev. *16*, 1291–1302.

Liu, Y., Shi, J., Lu, C.C., Wang, Z.B., Lyuksyutova, A.I., Song, X., and Zou, Y. (2005). Ryk-mediated Wnt repulsion regulates posterior-directed growth of corticospinal tract. Nat. Neurosci. *8*, 1151–1159.

Lu, W., Yamamoto, V., Ortega, B., and Baltimore, D. (2004). Mammalian Ryk is a Wnt coreceptor required for stimulation of neurite outgrowth. Cell *119*, 97–108.

Lyuksyutova, A.I., Lu, C.C., Milanesio, N., King, L.A., Guo, N., Wang, Y., Nathans, J., Tessier-Lavigne, M., and Zou, Y. (2003). Anterior-posterior guidance of commissural axons by Wnt-frizzled signaling. Science *302*, 1984–1988.

Maloof, J.N., Whangbo, J., Harris, J.M., Jongeward, G.D., and Kenyon, C. (1999). A Wnt signaling pathway controls hox gene expression and neuroblast migration in *C. elegans*. Development *126*, 37–49.

Manser, J., and Wood, W.B. (1990). Mutations affecting embryonic cell migrations in *Caenorhabditis elegans*. Dev. Genet. *11*, 49–64.

Mello, C.C., Kramer, J.M., Stinchcomb, D., and Ambros, V. (1991). Efficient gene transfer in *C. elegans*: extrachromosomal maintenance and integration of transforming sequences. EMBO J. *10*, 3959–3970.

Mitchell, K.J., Doyle, J.L., Serafini, T., Kennedy, T.E., Tessier-Lavigne, M., Goodman, C.S., and Dickson, B.J. (1996). Genetic analysis of Netrin genes in *Drosophila*: Netrins guide CNS commissural axons and peripheral motor axons. Neuron *17*, 203–215.

Rocheleau, C.E., Downs, W.D., Lin, R., Wittmann, C., Bei, Y., Cha, Y.H., Ali, M., Priess, J.R., and Mello, C.C. (1997). Wnt signaling and an APC-related gene specify endoderm in early *C. elegans* embryos. Cell *90*, 707–716.

Rulifson, E.J., Wu, C.H., and Nusse, R. (2000). Pathway specificity by the bifunctional receptor frizzled is determined by affinity for wingless. Mol. Cell *6*, 117–126.

Sagasti, A., Hobert, O., Troemel, E.R., Ruvkun, G., and Bargmann, C.I. (1999). Alternative olfactory neuron fates are specified by the LIM homeobox gene *lim-4*. Genes Dev. *13*, 1794–1806.

Salser, S.J., and Kenyon, C. (1992). Activation of a *C. elegans* Antennapedia homologue in migrating cells controls their direction of migration. Nature *355*, 255–258.

Schnorrer, F., and Dickson, B.J. (2004). Axon guidance: morphogens show the way. Curr. Biol. *14*, R19–R21.

Serafini, T., Kennedy, T.E., Galko, M.J., Mirzayan, C., Jessell, T.M., and Tessier-Lavigne, M. (1994). The netrins define a family of axon outgrowth-promoting proteins homologous to *C. elegans* UNC-6. Cell *78*, 409–424.

Tessier-Lavigne, M., and Goodman, C.S. (1996). The molecular biology of axon guidance. Science *274*, 1123–1133.

Thorpe, C.J., Schlesinger, A., Carter, J.C., and Bowerman, B. (1997). Wnt signaling polarizes an early *C. elegans* blastomere to distinguish endoderm from mesoderm. Cell *90*, 695–705.

Veeman, M.T., Axelrod, J.D., and Moon, R.T. (2003). A second canon. Functions and mechanisms of beta-catenin-independent Wnt signaling. Dev. Cell *5*, 367–377.

Wadsworth, W.G., Bhatt, H., and Hedgecock, E.M. (1996). Neuroglia and pioneer neurons express UNC-6 to provide global and local netrin cues for guiding migrations in *C. elegans*. Neuron *16*, 35–46.

Wang, B.B., Muller-Immergluck, M.M., Austin, J., Robinson, N.T., Chisholm, A., and Kenyon, C. (1993). A homeotic gene cluster patterns the anteroposterior body axis of *C. elegans*. Cell *74*, 29–42.

Wang, Y., Macke, J.P., Abella, B.S., Andreasson, K., Worley, P., Gilbert, D.J., Copeland, N.G., Jenkins, N.A., and Nathans, J. (1996). A large family of putative transmembrane receptors homologous to the product of the *Drosophila* tissue polarity gene frizzled. J. Biol. Chem. *271*, 4468–4476.

Whangbo, J., and Kenyon, C. (1999). A Wnt signaling system that specifies two patterns of cell migration in *C. elegans*. Mol. Cell *4*, 851–858.

Whangbo, J., Harris, J., and Kenyon, C. (2000). Multiple levels of regulation specify the polarity of an asymmetric cell division in *C. elegans*. Development *127*, 4587–4598.

White, J.G., Southgate, E., Thomson, J.N., and Brenner, S. (1986). The structure of the nervous system of the nematode *Caenorhabditis elegans*. Philos. Trans. R. Soc. Lond. B Biol. Sci. *314*, 1–340.

Wightman, B., Clark, S.G., Taskar, A.M., Forrester, W.C., Maricq, A.V., Bargmann, C.I., and Garriga, G. (1996). The *C. elegans* gene *vab-8* guides posteriorly directed axon outgrowth and cell migration. Development *122*, 671–682.

Wodarz, A., and Nusse, R. (1998). Mechanisms of Wnt signaling in development. Annu. Rev. Cell Dev. Biol. *14*, 59–88.

Wolf, F.W., Hung, M.S., Wightman, B., Way, J., and Garriga, G. (1998). *vab-8* is a key regulator of posteriorly directed migrations in *C. elegans* and encodes a novel protein with kinesin motor similarity. Neuron *20*, 655–666.

Wu, C.H., and Nusse, R. (2002). Ligand receptor interactions in the Wnt signaling pathway in *Drosophila*. J. Biol. Chem. *277*, 41762–41769.

Yoshikawa, S., McKinnon, R.D., Kokel, M., and Thomas, J.B. (2003). Wnt-mediated axon guidance via the *Drosophila* Derailed receptor. Nature *422*, 583–588.

Zecca, M., Basler, K., and Struhl, G. (1996). Direct and long-range action of a wingless morphogen gradient. Cell *87*, 833–844.